

Revealing the influence of Nb-doping on the crystal structure and electromechanical properties of (K, Bi)(Mg, Ti, Nb)O₃ ceramics

Aurang Zeb¹ · Fazli Akram² · Muhammad Habib³ · Qamar Iqbal⁴ · Amir Ullah¹ · Ihsan Ullah⁵ · Nasir Ali⁶ · S. J. Milne⁷ · Muhammad Sheeraz⁸ · Conrad Ingram² · Shahid Iqbal⁹ · Fayaz Hussain¹⁰ · Adnan Younis¹¹ · P. T. Tho¹² · Chang Won Ahn⁸

Received: 13 March 2023 / Accepted: 8 July 2023 / Published online: 18 July 2023 © The Author(s), under exclusive licence to Springer Science+Business Media, LLC, part of Springer Nature 2023

Abstract

Nb-modified lead-free ceramics ($K_{0.48}Bi_{0.52}$)($Mg_{0.02}Ti_{0.98-x}Nb_x$)O₃, (KBT-BMTNbx with x=0.00 – 0.05) were synthesized by a conventional solid-state reaction route followed by furnace cooling. The effects of Nb-doping on the structural properties and electrical properties of KBT-BMTNbx ceramics have been investigated. The X-ray diffraction pattern indicates a mixed tetragonal and cubic phase for the pure KBT-BMTNbx ceramics. Therefore, a large piezoelectric actuator coefficient $d_{33}^* \approx 700$ pm/V, piezoelectric sensor coefficient ($d_{33} \approx 133$ pC/N) along with remnant polarization ($P_r \approx 17.5 \, \mu \text{C/cm}^2$), maximum electromechanical strain $\approx 0.35\%$ and maximum temperature ($T_m \approx 336 \, ^{\circ}\text{C}$) were obtained for KBT-BMTNbx. However, with Nb-doping, a compositionally driven phase transformation occurred from mixed rhombohedral and tetragonal phases to cubic phase. Because of the excess Nb-doping in the KBT-BMT ceramics, the grain size suddenly decreased, as a result, the long-range ferroelectric phase was converted into a short-range relaxor phase. Hence, a low dielectric loss $tan\delta \approx 0.02$ was achieved at x=0.02 composition. This superior dielectric performance is correlated to the crystal structure morphotropic phase boundary, optimum grain size ($\approx 2 \, \mu m$), maximum lattice distortion, and soft-ferroelectric effect induced by the donor doping. The main aim of recent research is to investigate P_r , d_{33} , d_{33}^* , S_{max} , and reduced tan δ for practical applications in the real world.

Keywords Relaxor-ferroelectric · Lead-free ceramics · Nb-doping · KBT-BMT · Morphotropic phase boundary · Electromechanical properties

Aurang Zeb and Fazli Akram contributed equally to this work.

- Aurang Zeb a.zeb@icp.edu.pk
- Fazli Akram fazliakramss@gmail.com
- ☐ Chang Won Ahn cwahn@ulsan.ac.kr
- Department of Physics, Islamia College, Peshawar, KP, Pakistan
- Department of Chemistry, Clark Atlanta University, Atlanta, Georgia 30314, USA
- State Key Laboratory of Powder Metallurgy, Central South University, Changsha, Hunan 410083, China
- Department of Physics, Riphah International University, Islamabad 38000, Pakistan
- Department of Chemistry, Kyungpook National University, 80 Daehak-ro, Buk-gu, Daegu 41566, Republic of Korea

- Department of Physics, State Key Laboratory of Silicon Materials, Zhejiang University, Hangzhou 310027, China
- School of Chemical and Process Engineering, University of Leeds, Leeds LS2 9JT, UK
- Department of Physics and Energy Harvest-Storage Research Center (EHSRC), University of Ulsan, Ulsan 44610, Republic of Korea
- Department of Physics, University of Wisconsin-La Crosse, La Crosse, WI 54601, USA
- Department of Materials Engineering, NED University of Engineering and Technology, Main University Road, Karachi 75270, Pakistan
- Department of Physics, College of Science, University of Bahrain, Bahrain 32038, Kingdom of Bahrain
- Laboratory of Magnetism and Magnetic Materials, Science and Technology Advanced Institute, Faculty of Applied Technology, School of Technology, Van Lang University, Ho Chi Minh City, Viet Nam



1 Introduction

Because of its exceptional piezoelectric properties, lead zirconate titanate (PbZr₁ -xTi₂O₃, PZT) is employed in sensors, actuators, and transducers [1, 2]. The piezoelectric sensor coefficient (d_{33}), piezoelectric actuator coefficient (d_{33}^*) , and maximum temperature (T_m) are the desired parameters for piezoelectric ceramic devices in real-world applications [3, 4]. The piezoelectric sensor coefficient relation is $d_{33} = \sigma/E$, where σ mechanical stress and E is electrical energy. This refers to the sensitivity of a piezoelectric material to applied mechanical stress, resulting in an electrical output. It quantifies the relationship between the generated electrical charge and the applied mechanical force or pressure. On the other hand, the piezoelectric actuator coefficient $d_{33}^* = (S_{\text{max}}/E_{\text{max}})$, where S_{max} is the maximum strain obtained and corresponds to maximum field applied $E_{\rm max}$) represents the ability of a piezoelectric material to convert electrical energy into mechanical displacement or strain. It characterizes the magnitude of the mechanical response exhibited by the material in response to an applied electric field. Both coefficients are crucial parameters in understanding and evaluating the performance of piezoelectric materials for sensing and actuation applications [5–7]. Nevertheless, the environment and human health are negatively impacted by the free disposal of lead-based items [8, 9]. Therefore, lead-free piezoceramics development is a key parameter for the advancement of technology [10–12]. There have been many different materials used in the search for lead-free piezoelectric materials, the majority of which are based on the perovskite crystal structure [7, 13–16]. One of the most extensively investigated instances of alternatives to lead zirconate titanate (PZT) systems is the binary solid solutions based on sodium bismuth titanate Na_{1/2}Bi_{1/2}TiO₃ (NBT), $Na_{1/2}Bi_{1/2}TiO_3-BaTiO_3$ (NBT-BT), $Na_{1/2}Bi_{1/2}TiO_3$ and $K_{1/2}Bi_{1/2}TiO_3$ (NBT-KBT) [17–19], NBT-KBT-BaTiO₃ [20], NBT-KBT-SrTiO₃ [21], and KBT-based (1 $-x)K_{1/2}Bi_{1/2}TiO_3 - x Bi(Mg_{1/2}Ti_{1/2})O_3 (KBT-BMT)$ [22].

Large electromechanical strains, in the range 0.30–0.45% at electric field amplitudes of 80 kV/cm (bipolar) have been reported for NBT-based binary solid solutions, and hence these materials have been the subject of intense research activity. The maximum values of piezoelectric sensor coefficient d_{33} are reported to be in the range of 122–190 pC/N for NBT-based system near its morphotropic phase boundary (MPB) [23–25]. The NBT-based system display also inflections in plots of relative permittivity-temperature ($\epsilon_{\rm r}$ –T) well below the dielectric peak temperature: these infections are associated with depolarisation and loss of piezoelectric activity. For example, BNT-BT loses its piezoelectric properties at a depolarization temperature ($T_{\rm d} \approx 100$ °C) [25, 26]. At compositions close to 80NBT-20KBT, the system

is said to form a rhombohedral-tetragonal morphotropic phase boundary, providing an optimum piezoelectric performance with a d_{33} of 150 pC/N [17, 18]. Despite depolarization occurring at a lower temperature of 130 °C, it is a relaxor dielectric with $T_{\rm m} \approx 300$ °C. This restricts the maximum operating temperature of the piezoelectric device to \leq 130 °C, around 100 °C lower than most PZTs [20, 21, 27].

Therefore, until now, lead-free materials do not fulfill the requirement to replace lead-based ceramics in practical applications. From the materials design point of view, large piezoelectric, dielectric, and ferroelectric properties with high $T_{\rm m}$ are desired for industrial applications [28–30]. Therefore, it is a great need to develop eco-friendly piezoelectric ceramics with excellent electromechanical properties and high $T_{\rm m}$.

The solid solution between $K_{1/2}Bi_{1/2}TiO_3$ (KBT) and $Bi(Mg_{1/2}Ti_{1/2})O_3$ is another illustration of a Bi-containing perovskite with potential piezoelectric capabilities. In KBT-rich (1-y)KBT-yBMT (where y=0.04) ceramics, we have shown significant electromechanical strains. For compositions x=0.04 and 0.06, maximum strains of 0.3% at fields of 50 kV/cm and normalized strain ($S_{\rm max}/E_{\rm max}$, where $S_{\rm max}$ maximum electromechanical strain and maximum electric field $E_{\rm max}$) value values of 600 pm/V occur. At the transition between the tetragonal and pseudocubic phases, the ideal set of attributes can be found [31].

In the current research study, lead-free Nb-modified ceramics KBT-BMTNbx were synthesized by a solid-state reaction process. The main objective of the current study was to obtain ferroelectric polarization (maximum polarization $P_{\rm m}$, and $P_{\rm r}$), d_{33} , d_{33}^* , $S_{\rm max}$ and reduced tan (δ) with simultaneously elevated $T_{\rm m}$ in a single composition. The piezoelectric sensor coefficient, $d_{33} \approx 133$ pC/N and piezoelectric actuator coefficient, $d_{33}^* \approx 700 \text{ pm/V}$ occur in KBT-BMTNbx ceramic. The donor modification will improve the functional property of the KBT-BMTNbx ceramic and the concept presented here can be applied to the design of leadfree piezoelectric material for real-life applications. Additionally, because of their different valences, donor doping creates a local random field and favors the relaxor phase, which enhances the performance of piezoelectric strain. The crystal structure, microstructure, and electromechanical (dielectric, ferroelectric, and piezoelectric) properties were studied in detail. In this work, a significant correlation between electromechanical characteristics and structural properties was found.



2 Experimental method

In current research work, the lead-free Nb-modified $0.96K_{1/2}Bi_{1/2}TiO_3-0.04Bi$ (Mg_{1/2}Ti_{1/2}) O₃ ceramics were synthesized in the research laboratory according to the formula: $(K_{0.48}Bi_{0.52})$ $(Mg_{0.02}Ti_{0.98-x}Nb_x)$ O_3 , (KBT-BMTNbx)with x = 0.00 - 0.05) using conventional solid-state reaction method. The starting reagents used such as Nb₂O₅ (Sigma Aldrich, 99% purity, St. Louis, MO), K₂CO₃ (Sigma Aldrich, 99% purity), Bi₂O₃ (Sigma Aldrich, 99.9% purity), MgO (Alfa Aesar, 99.9% purity) and TiO₂ (Sigma Aldrich, 99.9% purity). The powders were weighed in accordance with the proper ratios after drying for an entire night at 250 °C. The powders were blended in isopropanol for 24 h in a ball mill using a zirconia grinding medium. The dry mixtures were then passed through a 300 µm nylon filter and calcined at 850 °C for 3 h in closed alumina crucibles with heating and cooling rates of 5 °C/min. The powders were milled one more for 24 h after calcination, and 1 weight% of a binder was added (Ciba Glascol HA4: Ciba Specialty Chemicals, Bradford, UK). Powders that had been sieved were compressed into pellets with a diameter of 10 mm and a thickness of about ~ 1.5 mm at 100 MPa in a steel die, then cold isostatic pressed at 200 MPa. The heat was applied at a rate of 50 °C/h to 550 °C, then 300 °C/h to sintering temperatures of 1050-1080 °C with a dwell time of 4 h. This process burned away the binder.

With the use of X-ray powder diffraction (XRD, Bruker D8, Cu, $K_{\alpha} \sim 1.5406 \text{ A}^{\circ}$) and a scan speed of 1°/min, the phase purity of crushed sintered pellets was examined. Using the X'pert Highscore Plus software, a refinement based on peak profile fitting was done to determine unit cell characteristics [32]. For three pellets of each composition, the densities of sintered ceramic pellets were calculated geometrically. Relative densities were then calculated by

from unit cell parameters and the anticipated cell contents. The sintered pellets were reduced to a thickness of about ~1 mm for electrical characterizations, and silver paste (Agar Scientific) was applied to both faces before being burned in a furnace at 550 °C for 10 min. Using an impedance analyzer (HP Agilent, 4192 A Hewlett Packard, Santa Clara, CA), the relative permittivity and dielectric loss tangents were determined from 25 to 600 °C at various frequencies. A Radiant Technologies LC precision analyzer (Radiant Technologies Inc., Albuquerque, New Mexico) and a contact-type displacement sensor (Millitron; Model 140), respectively, were used to record the polarization-electric field and strain-field responses at room temperature (frequency = 1 Hz).

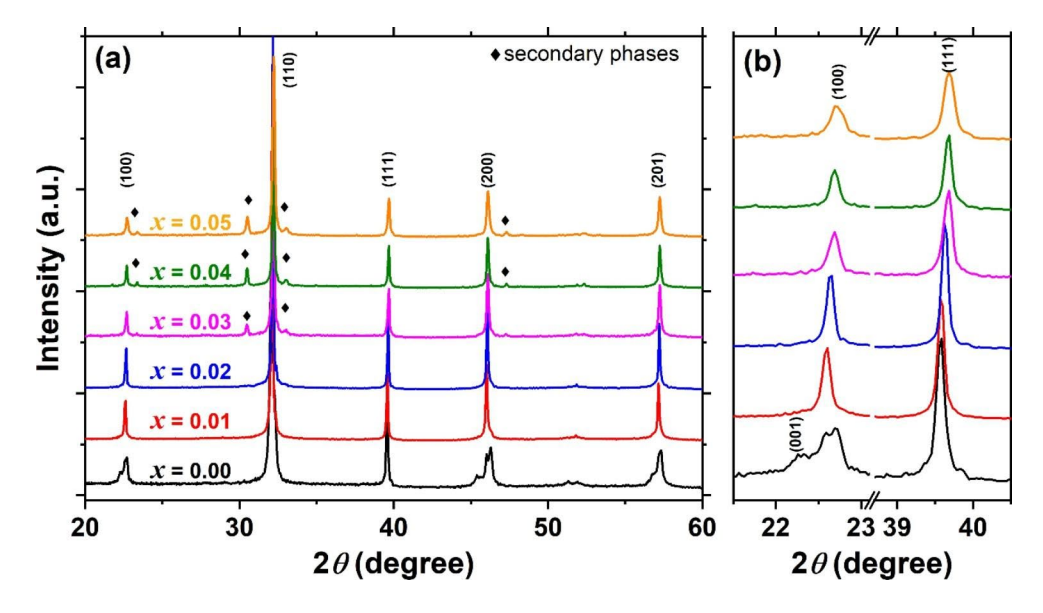
comparing these findings to theoretical densities calculated

3 Results and discussion

3.1 Structural properties

The XRD patterns for crushed sintered pellets of $(K_{0.48}Bi_{0.52})$ $(Mg_{0.02}Ti_{0.98-x}Nb_x)$ O_3 with $x\!=\!0.00-0.05$ ceramics at room temperature are depicted in Fig. 1. The XRD patterns show perovskite structure for $x\!\leq\!0.02$ with a mixed tetragonal plus pseudocubic perovskite phase. When Nb-content increased to $x\!=\!0.03$, an extra peak appeared in the perovskite structure. These extra peaks were identified as being due to bismuth titanate, $Bi_4Ti_3O_{12}$ [33, 34]. Regarding the appearance of $Bi_4Ti_3O_{12}$ as a second phase when the Nb content increased to $x\!=\!0.03$, it is important to note that the formation of additional phases can occur due to compositional changes and structural transformations. In this study, the increased Nb content led to a change in the local structure, resulting in the formation of $Bi_4Ti_3O_{12}$ as a secondary

Fig. 1 (a) XRD patterns for KBT-BMTNbx ceramics with x = (0.00 - 0.05) and (b) magnified view for the (111) and (100) peaks





phase. The specific mechanisms behind this phase formation are still under investigation and would require further analysis to provide a more detailed explanation. Thus, compositions x=0.03, 0.04, and 0.05 confirm that the crystal structure transforms into a single cubic phase.

Furthermore, the positions of the diffraction peaks in the Nb-doped KBT-BMT ceramics exhibit gradual variations compared to the parent KBT-BMT. Initially, the pure KBT-BMT ceramic displays two distinct peaks, namely $(001)_T$ and $(100)_T$, around 22.5° , and a single $(111)_R$ peak near 39.5° indicating a predominantly tetragonal (T) symmetry. However, with Nb-doping, these doubly split peaks gradually merge, along with the merging of $(1\ 1\ 1)$ and (111) peaks near 39.5° . This merging indicates a structural phase transition from a distorted tetragonal to a mixed tetragonal pseudocubic symmetry. Similar behavior has been reported for Pb substitution at the Bi site in BiFeO₃ [35]. Figure 1(b) provides an enlarged view of the range between 2θ of 22° and 23° , clearly demonstrating the merging of the (001) and (100) peaks.

To discuss in detail the lattice structure parameters, the crystal structure refinements were performed for Nb-doped KBT-BMT ceramics by using the biphasic structural model based on the R (R3c) and T (P4mm) phases for the crystal structure investigation. Figure 2 depicts the change in lattice parameters ($a_{\rm T}$, $c_{\rm T}$, and $a_{\rm C}$) of the samples with varying Nb-content levels. The tetragonal lattice parameters $a_{\rm T}=3.9083$ Å, $c_{\rm T}=3.9788$ Å, cubic lattice parameter $a_{\rm C}=3.9283$ Å, and tetragonality $c_{\rm T}/a_{\rm T}=1.018$ were used for pure samples.

Fig. 2 Lattice parameters for tetragonal (T) and cubic (C) phases as a function of *x* for KBT-BMTNb*x* ceramics

The introduction of Nb-doping, $a_T = 3.9286 \text{ Å}$, $c_T = 3.9398$ Å, $a_C = 3.9294$ Å, and $c_T/a_T = 1.003$ were used for x = 0.01compositions. The reduction in tetragonality suggests that the crystal structure is approaching the cubic-like phase because of the local structural heterogeneity induced by the Nb⁵⁺-donor doping. The increasing and decreasing developments of the lattice parameters of the crystal structure prove a good agreement with the XRD peak configuration. The cubic lattice parameters $a_C = 3.9350$ Å for composition x = 0.02 were changed into 3.9411 Å for x = 0.05 composition with slight variation. This indicates that the cubic phase becomes more prevalent at high Nb content in the KBT-BMT ceramics, and materials exhibit relaxor-ferroelectric behavior [36–38]. Chemical modification is a traditional method to customize the functional properties of the material. However, the selection of the base composition and chemical modifier is beneficial for improving their functional properties [39–41].

The SEM images demonstrate the effects of Nb concentration in KBT-BMT on the grain size and porosity of the samples. Figure 3 displays SEM micrographs for polished and thermally etched surfaces. The linear intercept approach was used to determine the grain size for each composition [42, 43]. The micrographs of each composition clearly indicate a somewhat dense structure, but the distribution of grain sizes is not uniform. In the case of the pure sample, the average grain size was estimated to be approximately 1 μ m, while for the sample with x=0.03, it was approximately 2 μ m. The compositions with x=0.03 exhibit dense

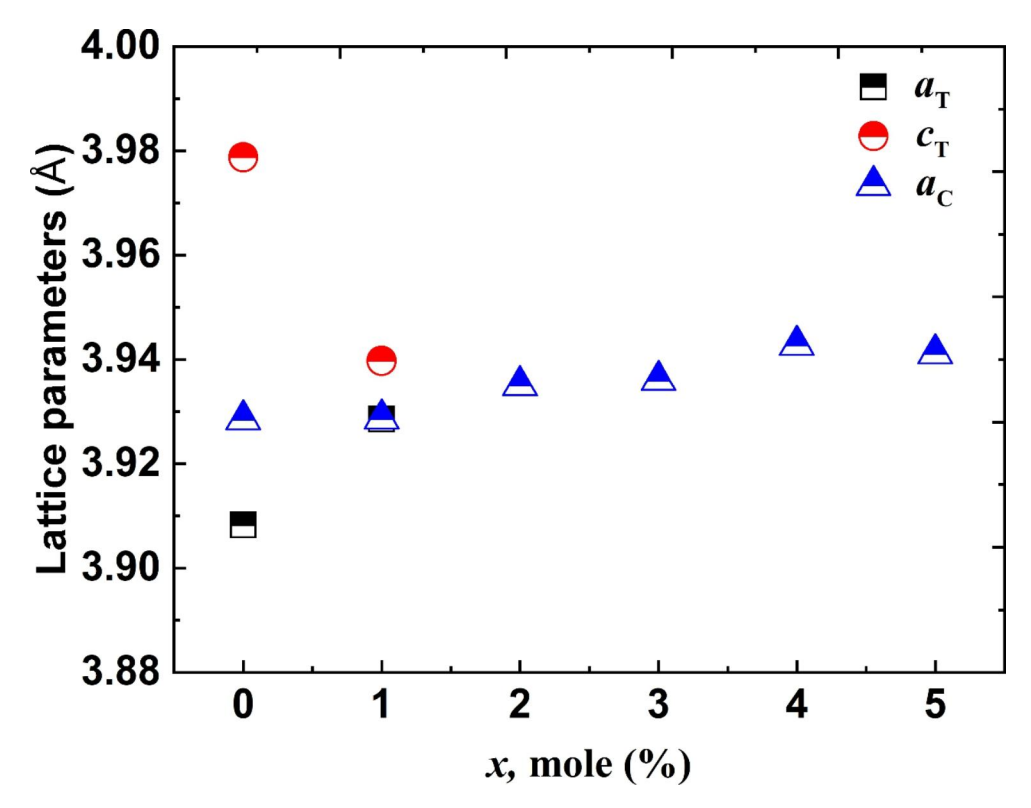
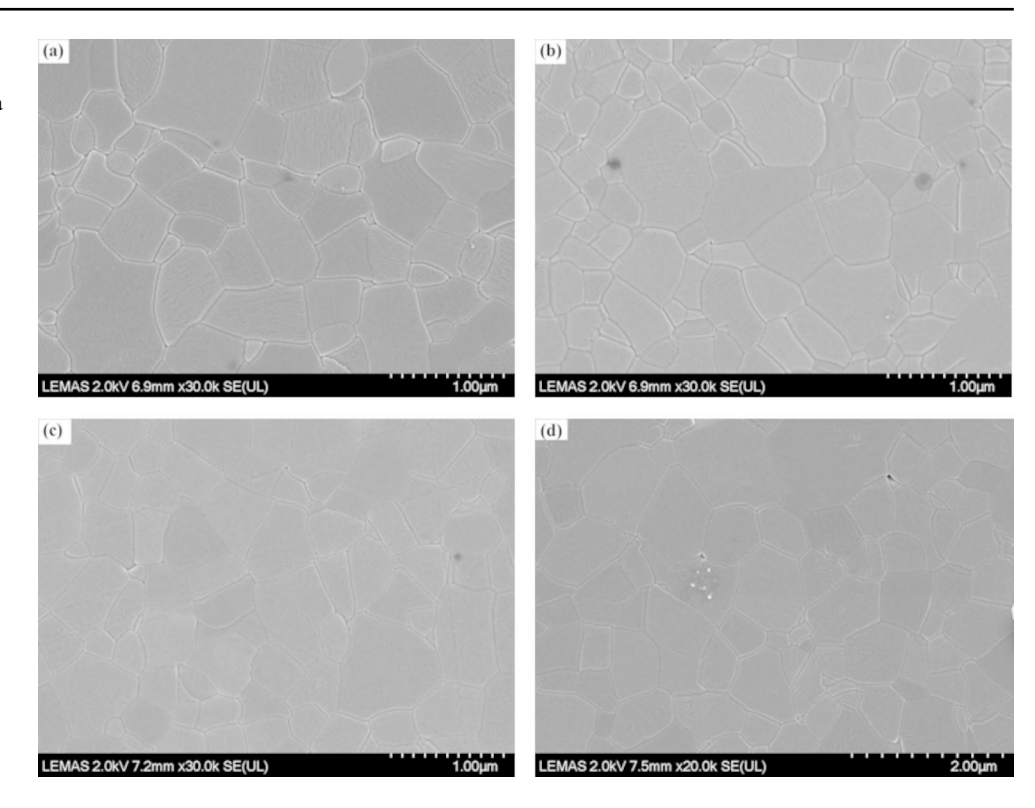




Fig. 3 (a-d) SEM micrographs of polished and thermally etched surfaces for x = (0.00 - 0.03) as a function of Nb-content



and compact microstructures, suggesting the potential for high electromechanical properties in this optimal composition. However, it should be noted that a few pores are present in this composition. Some literature reported that these pores may have formed due to the slow diffusion rate of Zr⁴⁺ (0.720 Å), which can be attributed to its larger ionic radius compared to Ti⁴⁺ (0.605 Å) [12, 44]. Furthermore, as the concentration of Nb increases, the grain size of KBT-BMT also increases, ranging from approximately 1 to 2 µm, as discussed before. This observation suggests that higher concentrations of Nb act as inhibitors for grain growth, possibly due to the more refractory nature of Nb₂O₃. It is worth noting that the grain size is significantly influenced by the sintering temperature and plays a crucial role in enhancing the ferroelectric, piezoelectric, and dielectric properties [45, 46]. Furthermore, the relative densities of all samples, determined using the Archimedes principle [47, 48], were found to be above 95%. Therefore, the microstructure evolution, including the average grain size and level of densification, was identified as one of the main key factors contributing to the improved electromechanical performance of ecofriendly ceramic materials.

3.2 Dielectric properties

The relative dielectric permittivity (ε_r) and tangent loss ($\tan \delta$) versus temperature measured at various frequencies are presented in Fig. 4. All sample compositions showed frequency dispersion typical of a relaxor-ferroelectric

[49–51]. The addition of Nb content, lowered the $T_{\rm m}$ and $\varepsilon_{\rm r}$. The results depicted in Fig. 5 indicate that the temperature at which the $T_{\rm m}$ and $\varepsilon_{\rm r}$ occur for the undoped ceramics were 336 °C and 6250, respectively. However, for the x = 0.03 composition, these values decreased to 240 °C and 2840, respectively, at a frequency of 1 kHz. The decrease in $T_{\rm m}$ observed could potentially be attributed to the presence of local structural heterogeneity or an increase in the disordering of A-site cations. This statement gains further significance when considering the remarkable characteristics of the unmodified KBT-BMT ceramic, which include an exceptionally high $T_{\rm m}$ and a significant $\varepsilon_{\rm r}$. However, with the introduction of Nb⁵⁺ doping, the temperature-dependent dielectric constant gradually becomes broader and shows frequency dispersion, indicative of a diffused phase transition characteristic of relaxor-ferroelectrics. This relaxor-like behavior can be attributed to atomic-scale local structure heterogeneity or domain miniaturization induced by the incorporation of La³⁺ as a donor dopant [52]. In previous studies on PZT ceramics, it has been reported that substituting the lone pair ion (Pb²⁺) with a non-lone pair ion (La³⁺) disrupts polar coupling, resulting in a shift of $T_{\rm m}$ towards lower temperatures [53]. Similarly, in KBT-BMT ceramics, it is plausible that the substitution of the lone pair ion (Bi³⁺) with the non-lone pair ion (Nb⁵⁺) weakens the lone pair activity, leading to a decrease in $T_{\rm m}$. This reduction in T_{m} flattens the thermodynamic energy profile and facilitates ferroelectric polarization switching under an applied



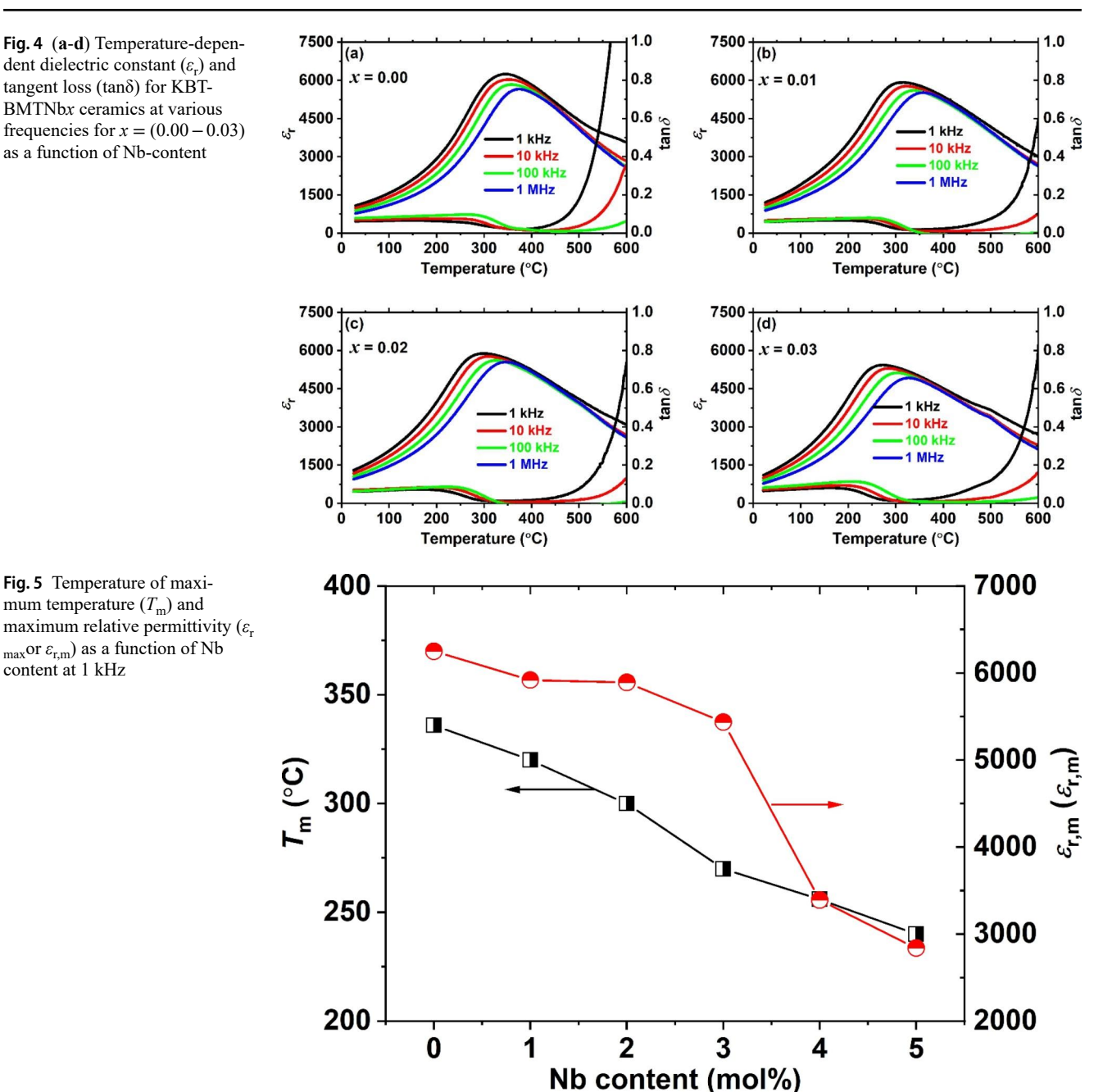
Fig. 4 (a-d) Temperature-dependent dielectric constant (ε_{r}) and tangent loss (tanδ) for KBT-BMTNbx ceramics at various frequencies for x = (0.00 - 0.03)as a function of Nb-content

Fig. 5 Temperature of maxi-

mum temperature (T_m) and

content at 1 kHz

 $_{max}$ or $\varepsilon_{r,m}$) as a function of Nb



electric field, ultimately contributing to the achievement of high piezoelectric performance [54].

For all fabricated ceramics compositions, Fig. 6 showed a linear increase with frequency for temperature, which corresponds to the maximum $\varepsilon_{\rm p}$ and $T_{\rm m}$. Temperature values for pure composition shifted from 340 °C at a frequency of 1 kHz to 375 °C at a frequency of 1 MHz. When Nb⁵⁺ was substituted in the ceramic system, similar trends for the growth of $T_{\rm m}$ with frequency increase were seen. At ambient temperature, the tan δ value for x = 0.02 composition was 0.06 and reduced to 0.02 at 350 °C. This suggests that losses are caused by space charge effects, which involve the migration of O vacancies in undoped materials [55–57]. Because Ti-ions are more highly polarizable than Mg and Nb-ions, then the lower value of ε_r may be the result of possible Ti-ion replacement by Mg and Nb-ions.

In order to validate the relaxor-ferroelectric behavior of the system, the degree of diffuseness factor (γ) was determined by analyzing the dielectric curves using the modified Curie-Weiss law [14, 58, 59]. In the case of normal ferroelectrics, the value of γ is typically 1, whereas, for relaxorferroelectrics, it tends to be closer to 2. By performing the calculations, we obtained γ values of 1.78, 1.70, 1.65, and 1.58 for compositions with x=0.00, 0.01, 0.02, and 0.03,



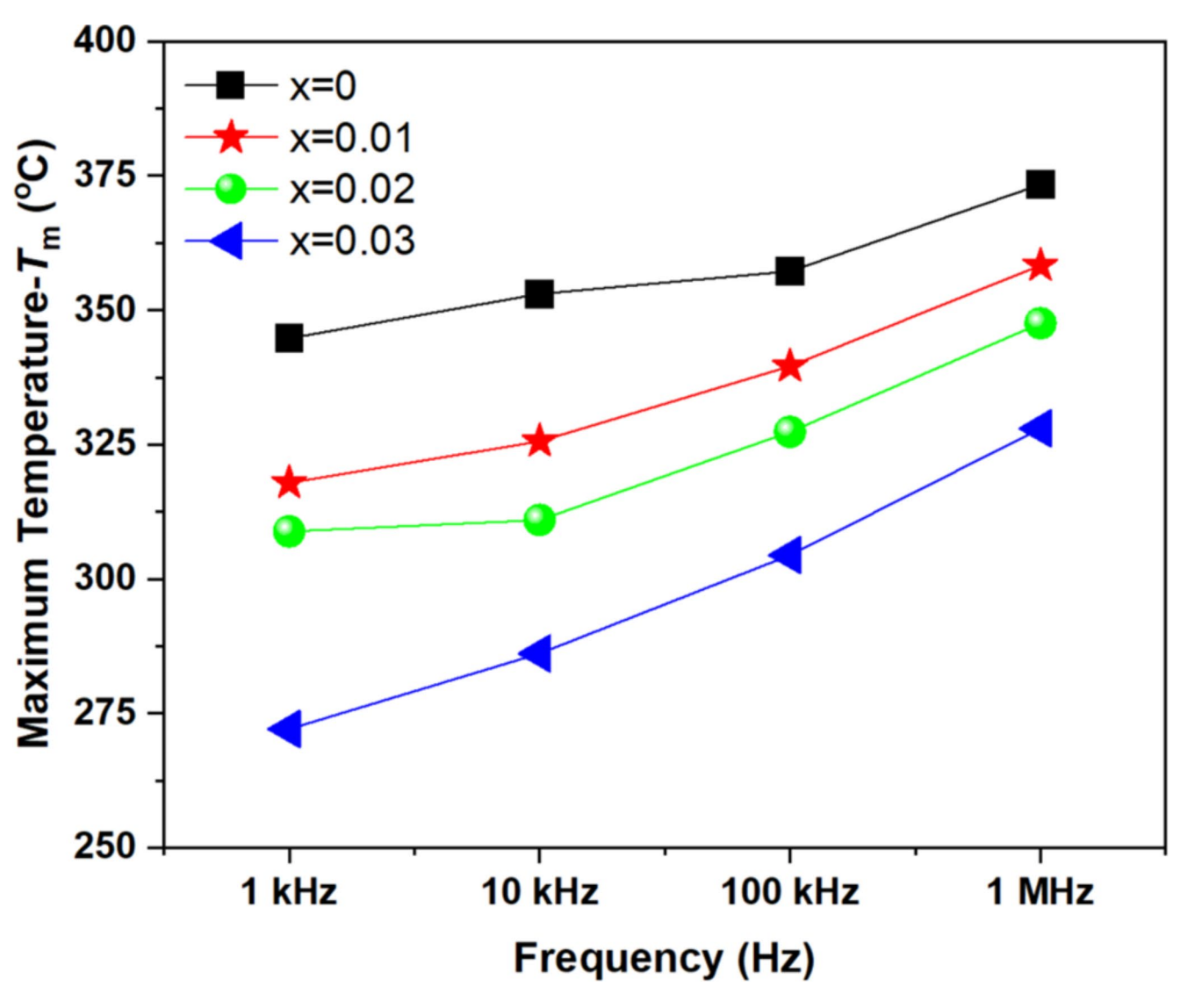


Fig. 6 Maximum temperature (T_m) as a function of frequency at different compositions (x = 0.00 - 0.03)

respectively. These values indicate a progressively decreasing degree of diffuseness, providing further evidence for the relaxor-ferroelectric behavior of the system.

3.3 Ferroelectric and piezoelectric properties

Figure 7 illustrates the polarization versus electric field (P-E) responses of ceramic materials measured at room temperature under an applied electric field of 50 kV/cm. The addition of Nb (KBT-BMTNb_x) noticeably influenced the polarization and coercive field of the base ceramics. The KBT-BMTNb_x ceramic with x=0.00 exhibited typical ferroelectric behavior, with a crystal structure located between mixed tetragonal and pseudocubic phases, as confirmed by XRD measurements. This resulted in a high $P_{\rm r}$, $P_{\rm m}$, and a large coercive field ($E_{\rm C}$). The pure sample displayed a wide lossy dielectric typical loop [8, 39, 40], indicating

ferroelectric behavior characterized by long-range order that preserves polarization after the removal of the applied electric field.

In contrast, the P-E loops in the Nb-doped samples became more constricted as the Nb concentration increased. Consequently, the P_r , P_m , and E_C values decreased (as shown in Table 1), indicating a transition towards a more characteristic relaxor-ferroelectric behavior. For example, the P_r values decreased from 14.28 μ C/cm² at x=0.01 to 5.76 μ C/cm² at x=0.05 composition, while the E_C decreased from 18.80 kV/cm to 10.70 kV/cm as x increased from 0.01 to 0.05 compositions. The P-E hysteresis loops became slimmer with Nb-doping, resulting in continuous decreases in both P_r and E_C . Consequently, the dominant long-range ferroelectric phase in undoped KBT-BMTNb $_x$ ceramics was disrupted by the presence of Nb, leading to the formation of a relaxor-ferroelectric phase. Additionally, at x \geq 0.01,



Fig. 7 The polarization versus electric field (P-E) loops at 10-60 kV/cm for Nb-doped BMTNbx (x=0.00, 0.01, 0.02, 0.03, 0.04 and 0.05) ceramics at 1 kHz

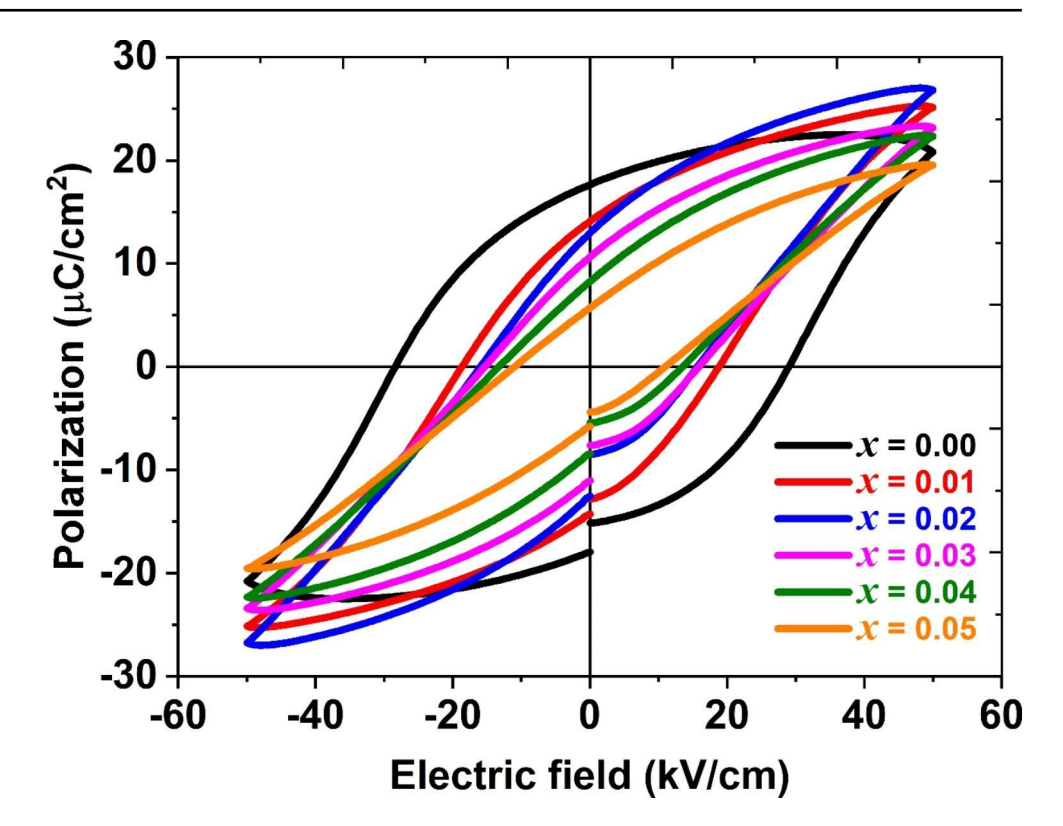


Table 1 Polarization hysteresis electrical parameters of $(K_{0.48}Bi_{0.52})$ $(Mg_{0.02}Ti_{0.08} - Nb.)$ O_3 with x = 0.01 - 0.0.05 ceramics

$(1150.02110.98-x^{1} \cdot 0x) \cdot 03 \text{ with } x = 0.01 \cdot 0.0.03 \text{ certaintes}$			
Composition (x)	$P_{\rm m} (\mu {\rm C/cm}^2)$	$P_{\rm r} (\mu {\rm C/cm}^2)$	E _C (kV/cm)
0.01	25.22	14.28	18.80
0.02	26.94	12.95	15.43
0.03	23.30	10.82	15.40
0.04	22.38	8.43	13.06
0.05	19.53	5.76	10.70

the formation of a relaxor-ferroelectric phase and pseudocubic phase contributed to a continuous decrease in the *P-E* hysteresis loops and dielectric constant of KBT-BMTNbx ceramics. Similar behavior has been previously reported in other BF-based ceramics [30, 60, 61].

The decrease in the $P_{\rm r}$, $P_{\rm m}$, and $E_{\rm C}$ with increasing Nb content in the KBT-BMT ceramics can be attributed to the disruptive influence of Nb on the dominant long-range ferroelectric phase. The incorporation of Nb likely leads to a conversion of the material towards a relaxor-ferroelectric phase, altering the crystal structure and overall ferroelectric properties. This disruption and conversion result in the observed reduction in P-E hysteresis loops and dielectric constant in the Nb-doped ceramics.

Figure 8 depicts the strain caused by an electric field for Nb-modified KBT-BMT ceramics with x=0.00-0.05. A typical butterfly shape loop with a noticeable negative strain (S_{neg}) was obtained for compositions at $x \le 0.03$ which is a characteristic of a ferroelectric material [62, 63]. However,

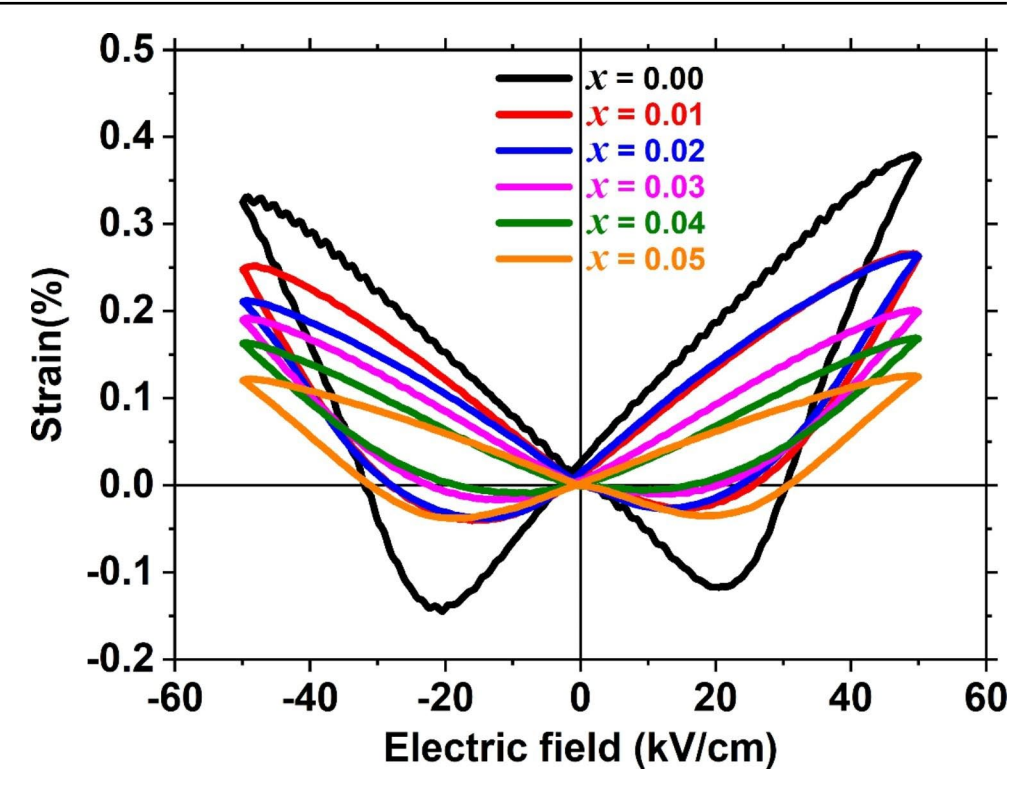
for $x \ge 0.04$ the $S_{\rm neg}$ is low, which indicates an increasing degree of relaxor contribution [64, 65]. The pure KBT-BMT ceramic reveals a high strain of ~0.35% at 50 kV/cm electric field. Electric field-induced strain values were lowered by the addition of Nb to just 0.25 and 0.12% at 50 kV/cm for x = 0.01 and 0.03 compositions, respectively. With further Nb inclusion, an electrostrictive response was produced with a maximum strain of 0.19% for x = 0.04.

In terms of practical applications, there has been significant research interest in the advancement of lead-free piezoelectric materials. This research primarily revolves around the exploration of solid solution systems that possess phase boundaries between distinct ferroelectric phases [25]. An extensively studied system in this regard is the binary solid solution between K_{1/2}Bi_{1/2}TiO₃ and Na_{1/2}Bi_{1/2}TiO₃ (KBT-NBT) [66]. They demonstrate that significant electromechanical strains and a high piezoelectric coefficient can be achieved at the intersection of the pseudocubic and tetragonal phases. The newly developed KBT-BMTNbx material exhibits large S_{max} and high d_{33}^* , making it a promising candidate for actuator and sensor applications at elevated temperatures. Consequently, the pure $(K_{0.48}Bi_{0.52})(Mg_{0.02}Ti_{0.98})O_3$ composition shows a large normalized strain $(S_{\text{max}}/E_{\text{max}})$ value of 700 pm/V even at a low electric field of 5 kV/mm.

To investigate the piezoelectric charge coefficient (d_{33}), the samples underwent poling in silicon oil baths at a temperature below 80 °C, while being subjected to an applied electric field ranging from 40 to 60 kV/cm. The obtained d_{33}



Fig. 8 The Electric field induced bipolar strain (S-E) curves of KBT-BMTNbx ceramics for compositions at x = 0.00 - 0.05



value was observed to be 133 pC/N for the x=0.00 composition, gradually decreasing to 23 pC/N with the increasing content of Nb, i.e. x=0.05. This finding is significant for the development of new materials with practical applications in various fields.

4 Conclusion

Using a traditional solid-state reaction method, we successfully synthesized a lead-free piezoelectric ceramics system known as $(K_{0.48}Bi_{0.52})(Mg_{0.02}Ti_{0.98-x}Nb_x)O_3$. Through X-ray diffraction (XRD) analysis at room temperature, we observed that the ceramic samples exhibited a mixed phase, combining both tetragonal and pseudocubic structures, for x values up to 0.01. However, as the Nb content increased to $x \ge 0.02$, a transition to a cubic structure occurred. Remarkably, our investigations revealed impressive properties for the KBT-BMTNbx composition. We achieved a large normalized strain value of 700 pm/V, indicating excellent piezoelectric performance. The piezoelectric sensor coefficient, d_{33} , was measured to be approximately 133 pC/N, and the remnant polarization (P_r) reached around 17.5 μ C/cm². Additionally, we obtained a maximum electromechanical strain of approximately 0.35% and a maximum temperature $(T_{\rm m})$ of approximately 336 °C. Furthermore, this study highlighted the effect of Nb content on dielectric loss ($tan\delta$). As the Nb content increased, the tanδ significantly decreased, dropping from 0.06 for x=0.00 to 0.02 for x=0.02 at a temperature of 350 °C. In addition, the maximum strain values were 0.35% for x=0.00 and 0.22% for x=0.02 composition were observed.

In summary, the main objective of our study was to achieve desirable properties, such as $P_{\rm r}$, d_{33} , d_{33}^* , $S_{\rm max}$, and reduced dielectric loss (tan δ), while simultaneously achieving an elevated $T_{\rm m}$, all within a KBT-based system. Our findings demonstrate the potential of the KBT-BMTNbx ceramic system for various practical applications in the field of piezoelectrics.

Author's contribution Dr. Aurang Zeb, Dr. Fazli Akram, Dr. Muhammad Habib, Dr. S.J. Milne, Dr. Amir Ullah, and Dr. Chang Won Ahn performed the experiment, analyzed the data, and prepare the first draft of the manuscript. Dr. Nasir Ali, Dr. Shahid Ali, Dr. Fayaz Hussain, Ihsan Ullah, and Qamar Iqbal helped with electromechanical properties measurements and their analysis. We express our gratitude to Dr. Muhammad Sheeraz, Dr. Conrad Ingram, Dr. Adnan Younis, and Dr. P.T. Tho for their valuable contributions to the revised manuscript. In addition, thanks to Dr. Aurang Zeb for sponsoring (HEC, Pakistan) and supervising this research work.

Funding and Acknowledgments Dr. Aurang Zeb thanks the Higher Education Commission of Pakistan and Islamia College Peshawar (Chartered University) for financial support. This was supported by the Higher Education Commission of Pakistan(HEC) grant funded by the National Research Program for Universities (NRPU) project No 10928. In addition, the National Science Foundation grant DMR-2122147 for the NSF-PREM Emergent Interface Materials Program between Clark Atlanta University, Spelman College, and Cornell University-PARADIM is also acknowledged.

Data Availability On request, all information and analysis are provided.



Declarations

Informed consent Not applicable.

Statement regarding research involving human participants and/or animals This article does not contain any studies with human or animal subjects.

Competing Interests There are no conflicts of interest that the authors are required to report.

References

- T. Yamada, T. Ueda, T. Kitayama, Piezoelectricity of a high-content lead zirconate titanate/polymer composite. J. Appl. Phys. 53, 4328–4332 (1982)
- R. Dittmer, K.G. Webber, E. Aulbach, W. Jo, X. Tan, J. Rödel, Optimal working regime of lead–zirconate–titanate for actuation applications. Sens. Actuators A: Phys. 189, 187–194 (2013)
- 3. G. Catalan, J.F. Scott, Physics and applications of bismuth ferrite. Adv. Mater. 21, 2463–2485 (2009)
- 4. F. Akram, R.A. Malik, T.K. Song, S. Lee, M.-H. Kim, Thermally-stable high dielectric properties of $(1-x)(0.65Bi_{1.05}FeO_3-0.35BaTiO_3)-xBiGaO_3$ piezoceramics. J. Eur. Ceram. Soc. **39**, 2304–2309 (2019)
- B. Wang, G. Huangfu, Z. Zheng, Y. Guo, Giant Electric Field-Induced strain with High Temperature-Stability in Textured KNN-Based Piezoceramics for Actuator Applications, Adv. Funct. Mater. (2023) 2214643
- F. Akram, A. Zeb, M. Habib, A. Ullah, P. Ahmad, S. Milne, A. Karoui, N. Ali, A. Kumar, S. Lee, Piezoelectric performance of the binary K_{1/2}Bi_{1/2}TiO₃-LiTaO₃ relaxor-ferroelectric ceramics. Mater. Chem. Phys. 279, 125764 (2022)
- B. Jaffe, W. Cook, H. Jaffe, Piezoelectric Ceramics (Academic Press, London and New York, 1971)
- Y. Saito, H. Takao, T. Tani, T. Nonoyama, K. Takatori, T. Homma, T. Nagaya, M. Nakamura, Lead-free piezoceramics. Nature. 432, 84–87 (2004)
- F. Akram, A. Hussain, R.A. Malik, T.K. Song, W.-J. Kim, M.-H. Kim, Synthesis and electromechanical properties of LiTaO₃-modified BiFeO₃-BaTiO₃ piezoceramics. Ceram. Int. 43, 209–213 (2017)
- M. Habib, F. Akram, P. Ahmad, F. Al-Harbi, I.U. Din, Q. Iqbal, T. Ahmed, S.A. Khan, A. Hussain, T.-K. Song, Donor multiple effects on the ferroelectric and piezoelectric performance of leadfree BiFeO₃-BaTiO₃ ceramics. Mater. Lett. 315, 131950 (2022)
- S. Zhang, R. Xia, T.R. Shrout, Lead-free piezoelectric ceramics vs. PZT? J Electroceram. 19, 251–257 (2007)
- F. Akram, R.A. Malik, A. Hussain, T.-K. Song, W.-J. Kim, M.-H. Kim, Temperature stable dielectric properties of lead-free BiFeO₃–BaTiO₃ modified with LiTaO₃ ceramics. Mater. Lett. 217, 16–19 (2018)
- J. Wu, Perovskite lead-free piezoelectric ceramics. J. Appl. Phys. 127, 190901 (2020)
- F. Akram, M. Habib, J. Bae, S.A. Khan, S.Y. Choi, T. Ahmed, S. Baek, S.T.U. Din, D.-H. Lim, S.-J. Jeong, Effect of heat-treatment mechanism on structural and electromechanical properties of eco-friendly (Bi, Ba)(Fe, Ti)O₃ piezoceramics. J. Mater. Sci. 58, 13198–13214 (2021)
- F. Akram, M. Sheeraz, A. Hussain, I.W. Kim, T.H. Kim, C.W. Ahn, Thermally-stable high energy-storage performance over a wide temperature range in relaxor-ferroelectric Bi_{1/2}Na_{1/2}TiO₃-based ceramics. Ceram. Int. 47, 23488–23496 (2021)

- T. Roncal-Herrero, J. Harrington, A. Zeb, S.J. Milne, A.P. Brown, Nanoscale compositional segregation and suppression of polar coupling in a relaxor ferroelectric. Acta Mater. 158, 422–429 (2018)
- O. Elkechai, M. Manier, J. Mercurio, Na_{0.5}Bi_{0.5}TiO₃–K_{0.5}Bi_{0.5}TiO₃ (NBT-KBT) system: a structural and electrical study, Phys. Status Solidi (a) 157 (1996) 499–506
- J.F. Li, K. Wang, F.Y. Zhu, L.Q. Cheng, F.Z. Yao, (K, Na) NbO₃-Based Lead-Free Piezoceramics: Fundamental Aspects, Processing Technologies, and Remaining Challenges, J. Am. Ceram. Soc. 96 (2013) 3677–3696
- T. Takenaka, H. Nagata, Y. Hiruma, Y. Yoshii, K. Matumoto, Lead-free piezoelectric ceramics based on perovskite structures. J Electroceram. 19, 259–265 (2007)
- H. Nagata, M. Yoshida, Y. Makiuchi, T. Takenaka, Large piezoelectric constant and high Curie temperature of lead-free piezoelectric ceramic ternary system based on bismuth sodium titanate-bismuth potassium titanate-barium titanate near the morphotropic phase boundary. Jpn. J. Appl. Phys. 42, 7401 (2003)
- F. Wang, C. Ming Leung, Y. Tang, T. Wang, W. Shi, Composition induced structure evolution and large strain response in ternary Bi_{0.5}Na_{0.5}TiO₃-Bi_{0.5}K_{0.5}TiO₃-SrTiO₃ solid solution. J. Appl. Phys. 114, 164105 (2013)
- A. Zeb, S.J. Milne, Large electromechanical strain in lead-free Binary System K_{0.5}Bi_{0.5}TiO₃-Bi(Mg_{0.5}Ti_{0.5})O₃. J. Am. Ceram. Soc. 97, 2413–2415 (2014)
- T. Takenaka, K.-i.M.K.-i., K.S.K. Maruyama, Sakata, (Bi_{1/2}Na_{1/2}) TiO₃-BaTiO₃ system for lead-free piezoelectric ceramics, Japanese journal of applied physics 30 (1991) 2236
- B.-J. Chu, D.-R. Chen, G.-R. Li, Q.-R. Yin, Electrical properties of Na_{1/2}Bi_{1/2}TiO₃–BaTiO3 ceramics. J. Eur. Ceram. Soc. 22, 2115–2121 (2002)
- J. Rödel, W. Jo, K.T. Seifert, E.M. Anton, T. Granzow, D. Damjanovic, Perspective on the development of lead-free piezoceramics. J. Am. Ceram. Soc. 92, 1153–1177 (2009)
- C. Ma, X. Tan, Phase diagram of unpoled lead-free (1 x)(Bi_{1/2}Na_{1/2}) TiO₃-xBaTiO₃ ceramics. Solid State Commun. 150, 1497–1500 (2010)
- A. Zeb, S.J. Milne, Large electromechanical strain in lead-free Binary System K_{0.5}Bi_{0.5}TiO₃-Bi (Mg_{0.5} Ti_{0.5})O₃. J. Am. Ceram. Soc. 97, 2413–2415 (2014)
- Y. Liu, Y. Chang, F. Li, B. Yang, Y. Sun, J. Wu, S. Zhang, R. Wang, W. Cao, Exceptionally high piezoelectric coefficient and low strain hysteresis in grain-oriented (ba, ca)(Ti, Zr) O3 through integrating crystallographic texture and domain engineering. ACS Appl. Mater. Interfaces. 9, 29863–29871 (2017)
- K. Wang, F.Z. Yao, W. Jo, D. Gobeljic, V.V. Shvartsman, D.C. Lupascu, J.F. Li, J. Rödel, Temperature-insensitive (K, na) NbO3-based lead-free piezoactuator ceramics. Adv. Funct. Mater. 23, 4079–4086 (2013)
- F. Akram, J. Kim, S.A. Khan, A. Zeb, H.G. Yeo, Y.S. Sung, T.K. Song, M.-H. Kim, S. Lee, Less temperature-dependent high dielectric and energy-storage properties of eco-friendly BiFeO₃–BaTiO₃-based ceramics. J. Alloys Compd. 818, 152878 (2020)
- A. Zeb, D.A. Hall, Z. Aslam, J. Forrester, J.-F. Li, Y. Li, C.C. Tang, G. Wang, F. Zhu, S.J. Milne, Structure-property relationships in the lead-free piezoceramic system K_{0.5}Bi_{0.5}TiO₃-BiMg_{0.5}Ti_{0.5}O₃. Acta Mater. 168, 100–108 (2019)
- 32. T. Degen, M. Sadki, E. Bron, U. König, G. Nénert, The highscore suite. Powder Diffr. 29, S13–S18 (2014)
- J. Dorrian, R. Newnham, D. Smith, M. Kay, Crystal structure of Bi₄Ti₃O₁₂, Ferroelectrics 3 (1972) 17–27
- A.D. Rae, J.G. Thompson, R. Withers, A.C. Willis, Structure refinement of commensurately modulated bismuth titanate, Bi₄Ti₃O₁₂. Acta Crystallogr., Sect. B: Struct. Sci. 46, 474–487 (1990)



- X. Zhang, Y. Sui, X. Wang, J. Tang, W. Su, Influence of diamagnetic pb doping on the crystal structure and multiferroic properties of the BiFeO₃ perovskite. J. Appl. Phys. 105, 07D918 (2009)
- B. Hu, M. Zhu, J. Guo, Y. Wang, M. Zheng, Y. Hou, Origin of relaxor behavior in K_{1/2}Bi_{1/2}TiO₃–Bi(Mg_{1/2}Ti_{1/2})O₃ investigated by electrical impedance spectroscopy. J. Am. Ceram. Soc. 99, 1637–1644 (2016)
- Q. Fan, C. Zhou, W. Zeng, L. Cao, C. Yuan, G. Rao, X. Li, Normal-to-relaxor ferroelectric phase transition and electrical properties in Nb-modified 0.72BiFeO₃-0.28BaTiO₃ ceramics. J Electroceram. 36, 1–7 (2016)
- P. Sun, H. Wang, X. Bu, Z. Chen, J. Du, L. Li, F. Wen, W. Bai, P. Zheng, W. Wu, Enhanced energy storage performance in bismuth layer-structured BaBi₂Me₂O₉ (me = nb and Ta) relaxor ferroelectric ceramics. Ceram. Int. 46, 15907–15914 (2020)
- K. Wang, A. Hussain, W. Jo, J. Rödel, Temperature-dependent Properties of (Bi_{1/2}Na_{1/2})TiO₃–(Bi_{1/2}K_{1/2}) TiO₃–SrTiO₃ lead-free Piezoceramics. J. Am. Ceram. Soc. 95, 2241–2247 (2012)
- F. Akram, R.A. Malik, S.A. Khan, A. Hussain, S. Lee, M.-H. Lee, C.H. In, T.-K. Song, W.-J. Kim, Y.S. Sung, Electromechanical properties of ternary BiFeO₃ – 0.35BaTiO₃–BiGaO₃ piezoelectric ceramics. J Electroceram. 41, 93–98 (2018)
- J.F. Li, K. Wang, F.Y. Zhu, L.Q. Cheng, F.Z. Yao, (K,na)NbO₃-based lead-free piezoceramics: fundamental aspects, processing technologies, and remaining challenges. J. Am. Ceram. Soc. 96, 3677–3696 (2013)
- 42. A. Thorvaldsen, The intercept method—2. Determination of spatial grain size. Acta Mater. **45**, 595–600 (1997)
- 43. H. Abrams, Grain size measurement by the intercept method. Metallography. **4**, 59–78 (1971)
- J. Wang, Y. Yu, S. Li, L. Guo, E. Wang, Y. Cao, Doping behavior of Zr⁴⁺ ions in Zr⁴⁺-doped TiO₂ nanoparticles. J. Phys. Chem. C 117, 27120–27126 (2013)
- J. Hao, W. Bai, W. Li, J. Zhai, Correlation between the microstructure and electrical properties in high-performance (Ba_{0.85}Ca_{0.15})(Zr_{0.1}Ti_{0.9})O3 lead-free piezoelectric ceramics. J. Am. Ceram. Soc. 95, 1998–2006 (2012)
- Z. Hanani, D. Mezzane, M. Amjoud, S. Fourcade, A.G. Razumnaya, I.A. Luk'Yanchuk, M. Gouné, Enhancement of dielectric properties of lead-free BCZT ferroelectric ceramics by grain size engineering. Superlattices Microstruct. 127, 109–117 (2019)
- M. Kireš, Archimedes' principle in action. Phys. Educ. 42, 484 (2007)
- 48. R. Benenson, Direct-reading archimedes' principle apparatus. Phys. Teacher. **13**, 366–366 (1975)
- D. Viehland, M. Wuttig, L. Cross, The glassy behavior of relaxor ferroelectrics. Ferroelectrics. 120, 71–77 (1991)
- F. Craciun, C. Galassi, R. Birjega, Electric-field-induced and spontaneous relaxor-ferroelectric phase transitions in (Na_{1/2}Bi_{1/2})₁₋, BaxTiO₃. J. Appl. Phys. 112, 124106 (2012)
- T.R. Shrout, J. Fielding, Relaxor ferroelectric materials, IEEE Symposium on Ultrasonics, IEEE, 1990, pp. 711–720
- M. Otonicar, A. Reichmann, K. Reichmann, Electric fieldinduced changes of domain structure and properties in La-doped PZT—From ferroelectrics towards relaxors. J. Eur. Ceram. Soc. 36, 2495–2504 (2016)
- 53. X. Chou, J. Zhai, H. Jiang, X. Yao, Dielectric properties and relaxor behavior of rare-earth (La, Sm, Eu, Dy, Y) substituted

- barium zirconium titanate ceramics. J. Appl. Phys. **102**, 084106 (2007)
- F. Li, D. Lin, Z. Chen, Z. Cheng, J. Wang, C. Li, Z. Xu, Q. Huang, X. Liao, L.-Q. Chen, Ultrahigh piezoelectricity in ferroelectric ceramics by design. Nat. Mater. 17, 349 (2018)
- M. Morozov, D. Damjanovic, Charge migration in Pb(Zr, Ti)O₃ ceramics and its relation to ageing, hardening, and softening. J. Appl. Phys. 107, 034106 (2010)
- A. Tian, R. Zuo, H. Qi, M. Shi, Large energy-storage density in transition-metal oxide modified NaNbO₃-Bi(Mg_{0.5}Ti_{0.5})O₃ leadfree ceramics through regulating the antiferroelectric phase structure. J. Mater. Chem. A 8, 8352–8359 (2020)
- 57. F. Yang, P. Wu, D.C. Sinclair, Suppression of electrical conductivity and switching of conduction mechanisms in 'stoichiometric' ($Na_{0.5}Bi_{0.5}TiO_3$)_{1-x}($BiAlO_3$)_x ($0 \le x \le 0.08$) solid solutions. J. Mater. Chem. C **5**, 7243–7252 (2017)
- Z. Yu, C. Ang, R. Guo, A. Bhalla, Ferroelectric-relaxor behavior of ba(Ti_{0.7}Zr_{0.3})O₃ ceramics. J. Appl. Phys. 92, 2655–2657 (2002)
- K. Uchino, S. Nomura, Critical exponents of the dielectric constants in diffused-phase-transition crystals. Ferroelectrics. 44, 55–61 (1982)
- T. Ahmed, S.A. Khan, M. Kim, F. Akram, H.W. Park, A. Hussain, I. Qazi, D.H. Lim, S.-J. Jeong, T.K. Song, Effective A-site modulation and crystal phase evolution for high ferro/piezoelectric performance in ABO₃ compounds: Yttrium-doped BiFeO₃-BaTiO₃. J. Alloys Compd. 933, 167709 (2023)
- D. Wang, G. Wang, S. Murakami, Z. Fan, A. Feteira, D. Zhou, S. Sun, Q. Zhao, I.M. Reaney, BiFeO₃-BaTiO₃: a new generation of lead-free electroceramics. J. Adv. Dielectr. 8, 1830004 (2018)
- H. Zhang, T. Wei, Q. Zhang, W. Ma, P. Fan, D. Salamon, S.-T. Zhang, B. Nan, H. Tan, Z.-G. Ye, A review on the development of lead-free ferroelectric energy-storage ceramics and multilayer capacitors. J. Mater. Chem. C 8, 16648–16667 (2020)
- N. Liu, R. Liang, Z. Zhou, X. Dong, Designing lead-free bismuth ferrite-based ceramics learning from relaxor ferroelectric behavior for simultaneous high energy density and efficiency under low electric field. J. Mater. Chem. C 6, 10211–10217 (2018)
- V.V. Shvartsman, D.C. Lupascu, Lead-free relaxor ferroelectrics.
 J. Am. Ceram. Soc. 95, 1–26 (2012)
- B. Qu, H. Du, Z. Yang, Lead-free relaxor ferroelectric ceramics with high optical transparency and energy storage ability. J. Mater. Chem. C 4, 1795–1803 (2016)
- 66. Y. Hiruma, K. Yoshii, H. Nagata, T. Takenaka, Phase transition temperature and electrical properties of (Bi_{1/2}Na_{1/2})TiO₃–(Bi_{1/2}A_{1/2})TiO₃ (A = Li and K) lead-free ferroelectric ceramics. J. Appl. Phys. 103, 084121 (2008)

Publisher's Note Springer Nature remains neutral with regard to jurisdictional claims in published maps and institutional affiliations.

Springer Nature or its licensor (e.g. a society or other partner) holds exclusive rights to this article under a publishing agreement with the author(s) or other rightsholder(s); author self-archiving of the accepted manuscript version of this article is solely governed by the terms of such publishing agreement and applicable law.

